7 Passive solar energy

Passive solar energy use supplies a significant contribution to the energy demand of every building, mainly by the short-wave solar irradiance transmitted by glazing, which is converted into heat by absorption on wall surfaces and provides daylight. Here that form of energy transfer is described as passive which takes place solely by thermal conduction, solar irradiance, long-wave radiation and free convection, i.e. is not line-bound and requires no auxiliary mechanical energy for moving a heat carrier.

Solar irradiance is absorbed without transport losses directly by the building shell or internal storage masses. Besides windows and the associated internal storage mass, the possibilities of passive use also include transparent thermal insulation on a heat-conducting external wall. Despite lower efficiency compared to windows, transparent thermal insulation in connection with a massive building component enables a temporal phase shift between irradiance and utilisation of heat, and so reduces the overheating problems of large glazings.

Unheated conservatories rank among the classical forms of passive solar use. As elements placed in front of the building shell they reduce, however, the direct solar irradiance through windows lying behind. Thus both the daylight and the direct heat entry into the adjoining heated rooms are clearly reduced. Furthermore, the indirect heating of glazed conservatories by adjoining rooms often leads to an increase in the heating requirement of buildings. Only with a very energy-conscious use of an unheated conservatory can energy gains for the building actually be achieved.

7.1 Passive solar use by glazings

Glazings are characterised by the fact that they display high transmittances for short-wave solar irradiance up to around 2.5 μm, but are impermeable to long-wave radiant heat emitted from building components with a maximum intensity of around 10 μm. The greenhouse effect results from this transmission and conversion of the solar irradiance by absorption in structural elements into heat, whose long-wave radiation proportion is not transmitted through the glazing.

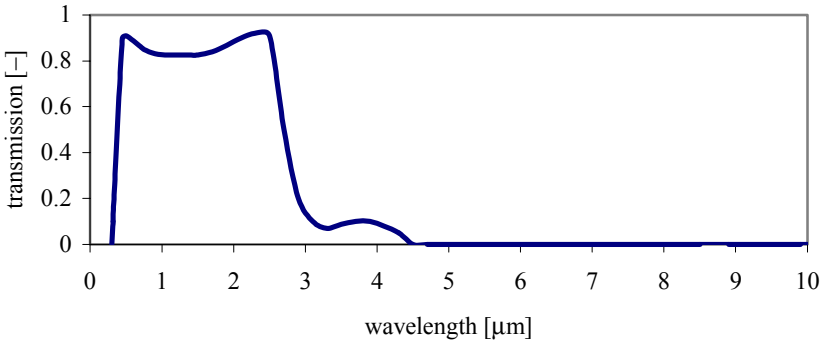

Figure 7.1: Wavelength-dependent transmittance of a single glazing.

7.1.1 Total energy transmittance of glazings

Apart from the direct transmission of the short-wave solar radiation with transmittance τ, part of the irradiance is absorbed in the panes, and by heating them causes a heat flow towards the room which contributes to the total energy transmission factor (g-value). The absorption coefficient of single glazing can be up to 30% for special sun-protection glazings. The secondary heat emission degree q_i is defined according to DIN EN 410 as the relation of the heat flow on the room side $\dot{Q}_i$ per square metre of window area A_w to the impacting solar radiation G, and calculated by solving heat balance equations. For each pane of a multi-pane system the degrees of transmission, absorption and reflection must be known. The total energy transmission factor then results from the relation of the total heat flow $\dot{Q}_{total}/A_w$ into the room to the irradiance:

$$g = \frac{\dot{Q}_{total} / A_w}{G} = \frac{\tau G + \dot{Q}_i / A_w}{G} = \tau + q_i \tag{7.1}$$

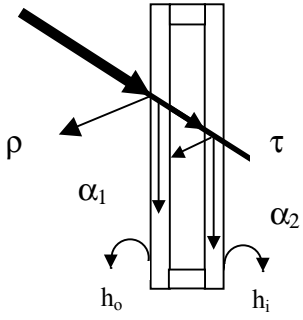

Figure 7.2: Transmission τ, reflection ρ, absorption α and heat transfer coefficients at the inside (h_i) and outside (h_o) of a double glazing.

The transmittance τ is calculated on the basis of DIN EN 410 by integration of the wavelength-dependent transmission over the solar spectrum. With perpendicular incidence it is approximately 90% for an uncoated simple float glass, and about 80% for a two-pane system. Due to today's commonly used metallic coating of the pane on the room side in thermally insulating glazing, the transmittance clearly falls, so the total energy transmission factor of the two-pane system is rarely over 65%. The absorption factor α of the short-wave solar radiation is likewise calculated for each pane by integration over the spectrum, and inter-reflections in multi-pane systems are taken into account.

The solutions of the heat balance equations for single, double and triple glazing are indicated in DIN EN 410. Using the example of single glazing, a heat balance can be described; the intensity αG absorbed by the pane of surface A_w is divided into a heat flow inward $\dot{Q}_i/A_w$ and outward $\dot{Q}_o/A_w$.

$$\alpha G = \frac{\dot{Q}_i}{A_w} + \frac{\dot{Q}_o}{A_w} \tag{7.2}$$

These heat flows can be calculated with the help of the heat transfer coefficients h_i (standard value 7.7 W/m^{2}K) and h_o (standard value 25 W/m^{2}K), and the temperature difference between pane surface T_s and room air T_i or outside air T_o. Temperature differences between the outside and inside surface are neglected.

$$\frac{\dot{Q}_i}{A_w} = h_i \left(T_s - T_i\right) \qquad \frac{\dot{Q}_o}{A_w} = h_o \left(T_s - T_o\right) \tag{7.3}$$

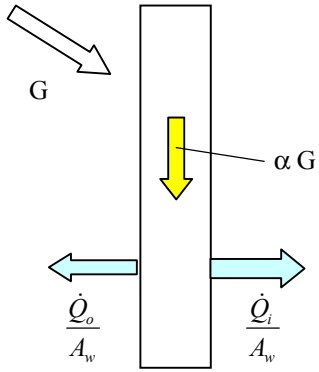

Figure 7.3: Irradiance G, absorption αG and secondary heat flows of single glazing outward and inward.

From the heat flow balance, first determine the pane surface temperature T_s:

$$\begin{aligned} \alpha G &= \left(h_i + h_o\right) T_s - h_i T_i - h_o T_o \\ \Rightarrow T_s &= \frac{\alpha G + h_i T_i + h_o T_o}{h_i + h_o} \end{aligned} \tag{7.4}$$

With this pane temperature T_s, the heat flow inward can be calculated:

$$\frac{\dot{Q}_i}{A_w} = h_i\left(T_s - T_i\right) = \frac{h_i}{h_i + h_o}\left(\alpha G - h_o\left(T_i - T_o\right)\right) = \underbrace{\frac{h_i}{h_i + h_o}\alpha G}_{\text{secondary heat flow}} \underbrace{- \frac{1}{\frac{1}{h_i} + \frac{1}{h_o}}\left(T_i - T_o\right)}_{\text{Transmission losses}} \quad (7.5)$$

Since the transmission heat losses of the glazing are calculated separately via the U-value, for the definition of the secondary heat emission degree q_i the ambient temperature can be set equal to the outside temperature. The result for q_i is:

$$q_i = \frac{\dot{Q}_i / A_w}{G} = \alpha \frac{h_i}{h_i + h_o} \quad \text{für } T_i = T_o \quad (7.6)$$

For double glazing the characteristic values are calculated accordingly, though for the outside pane a further heat balance must now be created. Defining the absorption coefficient for the outside pane as α_1 and for the internal pane as α_2, the secondary heat emission degree also depends on the layer thicknesses s_1, s_2 and heat conductivities λ_1, λ_2 of the two panes and on the thermal resistance R_{air} of the standing air layer between the panes:

$$q_i = \frac{\left(\frac{\alpha_1 + \alpha_2}{h_o} + \frac{\alpha_2}{\frac{s_1}{\lambda_1} + R_{air} + \frac{s_2}{\lambda_2}} \right)}{\frac{1}{h_i} + \frac{1}{h_o} + \frac{s_1}{\lambda_1} + R_{air} + \frac{s_2}{\lambda_2}} \quad (7.7)$$

The solar radiation let through (transmitted by) the glazing into the room $\dot{Q}_{trans}$ results directly from the product of the g-value and the solar irradiance:

$$\dot{Q}_{trans} = g\,G \quad (7.8)$$

7.1.2 Heat transfer coefficients of windows

The calorific losses through the window are deducted from the transmitted power, which are characterised by the heat transfer coefficient of the glazing U_g, or of the entire window including the frame U_w. Double glazing coated and filled with heavy noble gases achieve a minimum U_g value of 1.0 W/m^{2}K, triple glazing at best a U_g value of 0.4 W/m^{2}K. Even at a glazing U_g value of 1.3 W/m^{2}K, a wooden or plastic frame increases the window's U_w value slightly. For passive house concepts, specially insulated expanded polystyrene frameworks must be used, so that the low glazing values of triple glazing are not worsened by the frame proportion.

The passive solar gain $\dot{Q}_u$ usable in the room results from the balance of losses and gains. The losses are calculated from the U_w value of the window of surface A_w and from the temperature difference between the room air T_i and the outside air T_o:

$$\frac{\dot{Q}_u}{A_w} = U_w \left(T_i - T_o\right) - g\,G \tag{7.9}$$

From the available energy balance, an effective U-value U_{eff} can be defined, which is often used for monthly or annual balance calculations with mean temperature differences and irradiances.

$$U_{eff} = \frac{\dot{Q}_u}{A_w \left(T_i - T_o\right)} = U_w - g\frac{G}{T_i - T_o} \tag{7.10}$$

Balanced over a heating season, about 400 kWh/m^{2}a of solar irradiance is available on a south-facing facade in Germany. The mean temperature difference between the inside and outside of about 17°C, multiplied by the number of days in the heating season, results in the so-called heating degree day number, which on average in Germany is about 3500 Kelvin-days per year. The maximum usable energy per square metre of glazing surface for two-pane low-e coated glazing with a U_w value of 1 W/m^{2}K and $g = 0.65$ is thus:

$$\begin{aligned}\frac{Q_u}{A_w} &= 0.65 \times 400 \times 10^3 \frac{Wh}{m^2 a} - 1.0 \frac{W}{m^2 K} \times 3500 \frac{K\ days}{a} \times 24 \frac{h}{day} \\ &= 260 \frac{kWh}{m^2} - 84 \frac{kWh}{m^2} = 176 \frac{kWh}{m^2}\end{aligned} \tag{7.11}$$

The amount of heat effectively usable in the room depends greatly, however, on the storage capability of the structural elements on the inside, since high passive solar heat gains can easily lead to overheating of the interior and thus do not contribute to covering the heating requirement. A detailed analysis of the dynamic storage behaviour of building elements can be found in section 7.3.

In the monthly balance procedure based on EN 832 for calculating the heating requirement, the efficiency of the solar irradiance transmitted by windows is indicated as a function of the relation of the monthly gains to the transmission and ventilation heat losses. For low energy buildings with an annual heating requirement between about 30 and 70 kWh/m^{2}a the result is, for a heat-storing heavy building construction, a flat minimum of the heating requirement for a window area proportion on the south-facing facade of approximately 25%. In administrative buildings with mostly higher internal loads, the window area proportion should be lower still, to avoid overheating in summer. With a light building method with a small storage capacity, the minimum heating requirement is obtained for 0–20% of the window area proportion.

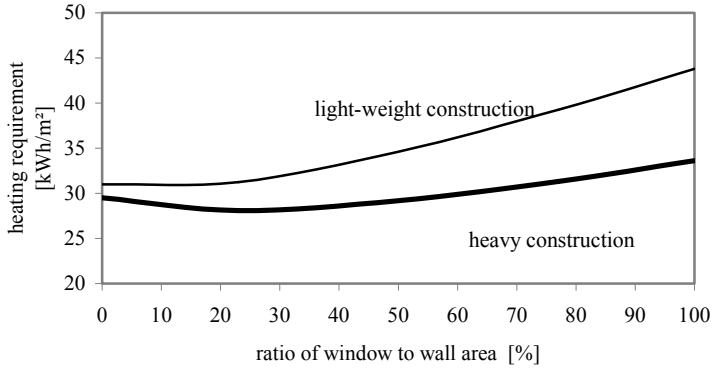

Figure 7.4: Influence of the window area proportion on the heating requirement.

7.1.3 New glazing systems

For flexible control of total energy transmission, glazing systems are being developed which modify their transparency degree temperature-dependently (thermo-tropic) or electrically controlled (electro-chromic).

Thermotropic layers are polymer mixtures or hydrogels which are inserted in a homogeneous mixture between two window panes, and which with rising temperature reduce the light permeability by up to 75% (Hartwig, 2000).

Electrochrome thin films, for example from tungsten oxide, are evaporated on window panes with conductive oxide coatings. On accumulation of cat-ions (e.g. Li+) from the counter-electrode to the tungsten oxide by an external electrical field, the transmittance falls wavelength-dependently to 10-20%. The two thin film electrodes are connected by a polymer ion conductor. A tight sealing at the edges is very important for long-term stability. With the first commercially available glasses with a maximum surface of 0.9 m × 2.0 m, a reduction of the total energy transmission factor from 44% in the bright status to 15% in the dark status is achieved (U-value = 1.6 W/m^{2}K) (Wittkopf *et al*., 1999); in systems with a lower U-value of 1.1 W/m^{2}K, the g-value falls from 36% to 12%.

7.2 Transparent thermal insulation

Since the early 1980s, several thousand square metres of transparent thermally insulated facade systems have been installed in Germany. Compared to conventional thermal insulation in buildings, transparently insulated external walls can use the incoming solar radiation to a far greater extent. The energy potential for the application of such solar systems is high; if a fifth of all existing facades were equipped with transparent insulating systems, approximately 15% of the heat needed for room heating could be supplied (Braun *et al*., 1992). The technology is particularly interesting for the renovation of old buildings with heavy, very heat-conducting walls (Eicker, 1996). Transparent insulated panes can be stuck directly on the external wall; a transparent plaster protects the material from the weather. By foregoing complex frame constructions, the costs of glass composite

structures, high so far, can be significantly reduced. A further application of transparent thermal insulation is daylighting. The light scattering and light directing by the elements can be used for an even illumination of the room, and the very good heat-insulating characteristics allow large-scale application on external walls.

7.2.1 Operational principle

If short-wave solar radiation hits an external wall, the radiation is absorbed and converted into heat. The external surface warms up, but most of the heat produced is mainly transferred to the outside air. Only a small part of the heat reaches the building interior. If a transparent insulating layer is attached in front of the wall (in the simplest case a window pane), heat emission to the outside is made more difficult.

The main parametres influencing the extent of the useful heat gain are the transmission coefficient for solar radiation and the heat resistance of the transparent thermal insulation on the one hand, and the absorption coefficient, heat conductivity and storage capability of the adjoining wall on the other. A time delay in the heat flow takes place due to the wall, so the maximum values of the solar-induced heat flow reach the inside when the direct solar gains through the windows have already decreased and outside temperatures are falling. In addition, the thermal characteristics of the entire building play a role, above all the heat-storing capability of the interior structural elements in avoiding overheating.

An external wall which even with 10 cm external insulation still has calorific losses of over 30 kWh per square metre and heating season, becomes a solar collector due to a transparent thermal insulation and produces around 50–100 kWh/m^2 of useful heat for the building.

The heat transition coefficient of an external wall insulated with TWD results as usual from the total of the thermal resistances of the existing external wall and the transparent insulation,

$$U_{eff} = U_{wall+TWD} - \eta_0 \frac{G}{T_i - T_o} \tag{7.12}$$

with layer thickness s_{TWD} and heat conductivity λ_{TWD} of the transparent insulating material, layer thickness s_{wall} and heat conductivity λ_{wall} of the external wall and also the heat transfer coefficients inside h_i and outside h_o.

The absorber is characterised by the absorption coefficient α, the transparent insulation by the diffuse total energy transmission factor g_d. The U-values of 10 cm TWD are typically about 0.8 W/m^{2}K, lower than the best double-glazed heat-protection glass, but still twice as high as the heat transfer coefficients of 10 cm of conventional insulating material with U-values of 0.4 W/m²K.

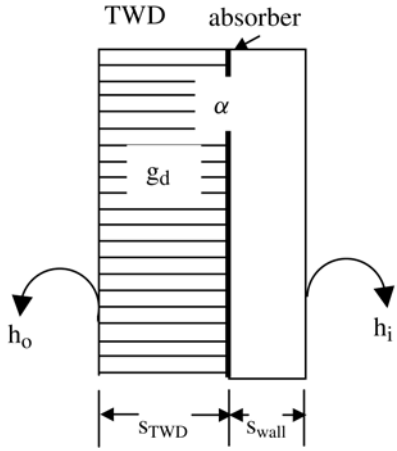

Figure 7.5: System structure of a transparently insulated wall.

Just as with the energy balance of windows, an effective U-value can also be defined for transparent thermal insulation as the difference between losses and solar gains with efficiency η_0.

$$U_{eff} = U_{wall+TWD} - \eta_0 \frac{G}{T_i - T_o} \tag{7.13}$$

Solar efficiencies η_0 up to 50% with a simultaneous low heat transfer coefficient lead to effective U-values which, with a favourable wall orientation, are negative on the annual average and thus are heat gains for the building. Measurements of a 10 cm transparently insulated building in Freiburg/Germany resulted in weekly averaged effective U-values between 0 and –3.5 W/m^{2}K.

The solar efficiency η_0 corresponds to the total energy transmission factor of a glazing and consists of the g_d-value of the transparent insulating material, the absorption factor of the absorber α and the proportion of the heat flow inward to the total heat flow. The heat flow from the absorber inward is calculated from the temperature node of the absorber at temperature T_a to the room air temperature T_i via the heat transfer coefficients of the wall $U_{wall} = \left(\frac{s_{wall}}{\lambda_{wall}} + \frac{1}{h_i} \right)^{-1}$:

$$\frac{\dot{Q}_i}{A} = U_{wall} \left(T_a - T_i \right) \tag{7.14}$$

The total heat flow results from the total heat flow inward (Equation (7.14)) and the heat flow from the absorber outward $\dot{Q}_o$, which is calculated via the heat transfer coefficient U_{TWD} of the TWD material:

$$\frac{\dot{Q}_o}{A} = U_{TWD}\left(T_a - T_o\right) \tag{7.15}$$

$$\eta_0 = \alpha g_d \frac{U_{wall}\left(T_a - T_i\right)}{U_{wall}\left(T_a - T_i\right) + U_{TWD}\left(T_a - T_o\right)} \tag{7.16}$$

Assuming identical temperatures inside and outside, a constant solar efficiency can be defined which is very suitable for material comparisons and estimates of the energy yield.

$$\eta_0 = \alpha g_d \frac{U_{wall}}{U_{wall} + U_{TWD}} \tag{7.17}$$

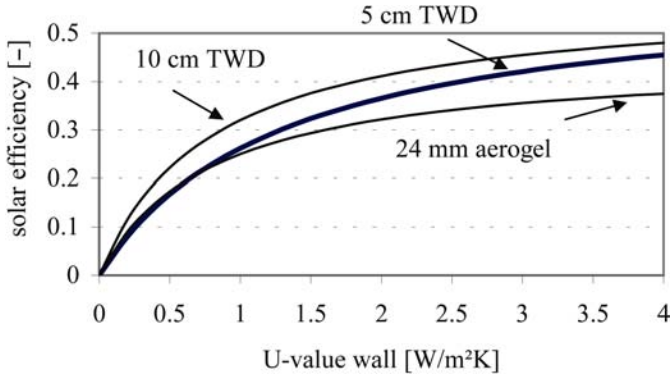

Figure 7.6: Solar efficiency as a function of the heat transfer coefficient of the opaque wall.

With 5 cm TWD capillaries, the U_{TWD} value is 1.3 W/m^{2}K at a g-value of 0.67; with 10 cm it is 0.8 W/m^{2}K and g = 0.64. The aerogel material shows a U_{TWD} value of 0.8 W/m^{2}K with a very small layer thickness of 2.4 cm at a g-value of 0.5.

For optimal use of solar heat, one must ensure that the transparently insulated room is not overheated. Conventional window areas usually bring sufficiently high solar gains into the room during the day; additional gains from the TWD wall must be stored and then used in the evening hours. The temporal shift between heat production at the absorber and maximum heat flow into the room rises with external wall thickness and also depends on the density, thermal capacity and heat conductivity of the wall. With a 24 cm brick or

lime-sandstone wall, phase shifts of 6 to 8 hours are achieved; with concrete walls, little more than 5 hours are possible. With sufficiently strong wall constructions, the result is typically 100% efficiencies of the heat produced by the TWD wall within the core months of the heating season; in the transition months around 30% (Wagner, 1998).

The high absorber temperatures of the external wall, which can reach peak values between 70° and 80°C, are effectively dampened at wall thicknesses over 20 cm and are, at the interior surface, rarely higher than 30°C even in the summer. The absorber temperatures are lower with heavy, heat-conducting components than with light walls with densities of around 800 kg/m³. The heat which develops can penetrate quickly into the heavy external wall and be led into the interior. Any thermal tensions are thus correspondingly low.

At an experimental house in Stuttgart the thermal deformations of the external wall were measured on a long-term basis. Compression stresses and slight swelling of the wall due to the high temperature difference did not pose a problem. Fine cracks of about 1 to 2 mm in the plaster resulted from accelerated drying of the new building's brickwork dampness around the absorber; they did not, however, influence the load-carrying capacity of the wall. With new buildings it is worth planning for defined joints at the edges of the TWD surfaces.

The use of shading systems such as blinds or shutters prevents heating of the external wall in the transition period and in the summer months, but it is complex in terms of construction and maintenance issues. Constructional shadings such as balconies or roof projections must be planned very carefully, in order not to obstruct exposure to the sun in the transition period. Foregoing shading mechanisms is possible if the transmittance of the transparent insulation is strongly angle-dependent, so that with a high sun position in the summer with angles of incidence over 60° at the south-facing facade, less than 20% of the irradiance reaches the absorber wall. The transmittance of a transparent heat insulation system falls, for example, from approximately 50% with perpendicular incidence to 15% with a sun elevation angle of 60°.

Simulations for highly insulated low-energy buildings have shown that even when the south-facing facade is largely covered with a TWD heat insulation system, the excess heat in summer can be expelled by night ventilation (Meyer, 1995). The number of hours with ambient temperatures over 26°C is fewer than 50 over the reference building with conventional insulation and is altogether below 300 hours per year.

On the other hand, at angles of incidence of 60°, capillary material with a glass covering displays a very high total energy transmission factor of 35%. In this case, sun protection is unavoidable, when the facade is largely covered. If nocturnal ventilation is not possible, e.g. in office buildings, shading of the TWD surfaces in the summer should likewise be provided for.

The orientation of the transparently insulated facade is crucial both for energy gain in the winter and for protection against overheating in the summer. Facade orientations between south-east and south-west are suitable. Twice as much energy, some 400 kWh/m^2, falls on a south-facing facade in the heating season as on an east or west-facing one. In addition, the low winter sun position leads to good light transmission by the TWD material. In summer, on the other hand, only the south-facing facade offers a certain natural sun protection with low transmittance.

7.2.2 Materials used and construction

TWD capillary or honeycomb structures are assembled from thin-walled plastic tubes and welded by a hot wire section or manufactured into strips of any width from extruder nozzles with an almost square cell cross-section. The typical cell diametre is 3 mm.

Two polymer types are in use today: Polymethyl methacrylates (PMMA) and polycarbonates (PC). PMMA is characterised by high transmittance and by good UV stability. Due to the brittleness of the material and its poor fire-retardance (class B3), PMMA is bound between window panes. For this, a qcomplex mullion-transom construction is necessary, leading to system costs between 400–750 €/m^2. The cost of the 10–12 cm transparent insulation is typically only around 50 €/m^2; it is the glazing and attachment, at approximately 250 €/m^2, plus shading items such as blinds at around 150 €/m^2, which drives up the costs.

Polycarbonates are mechanically more stable and can also be processed without glass covering; they are, however, not very UV-resistant. Their fire retardance is better (class B1) and the material is temperature-resistant to about 125°C. Polycarbonate materials can be used in heat insulating compound systems. The covering plaster is an acryl adhesive mixed with 2.5–3 mm diametre glass balls, which is applied in the factory directly onto the capillary material. Additional UV absorbers can be likewise brought into the cover plaster. Such heat insulating compound systems can be manufactured with substantially reduced costs of around 150 €/m^2, since there are no complex glazing and shading systems. The weight of capillary materials is around 30 kg/m^3.

Capillaries made of glass are manufactured like the polymer structures, but are complicated to produce due to high processing temperatures and the associated engineering problems. Glass capillaries are much more temperature- and UV-resistant, but likewise mechanically not very stable. The recycling ability of glass, which is also possible with PMMA, is advantageous. Polycarbonates, on the other hand, are recyclable only with high energy expenditure and with quality losses.

For glazing systems with smaller thicknesses of 2–3 cm, aerogels are suitable. These are highly porous, open-pored solids consisting of more than 90% air and 10% silicate, with very low heat conductivity (λ = 0.02 W/mK). Aerogels are made of silica gel and can easily be poured into the cavity of double glazing. They are not inflammable, are easy to dispose of and to recycle. The significant disadvantage is that their light transmission is only around half that of capillary materials, and their sensitivity to water is also a problem. Water penetrating into the edge network of double glazing is absorbed by the aerogel material and the sensitive structure is broken by the capillary forces.

7.2.2.1 Construction principles of TWD systems

Transparent heat insulating systems are mainly used in two types of construction:

1. as a mullion-transom or element construction with framed TWD panel elements. To avoid dirtying of the TWD materials, the external covers usually consists of two highly transparent, iron-poor single glass panes. Element constructions are characterised by a higher degree of prefabrication with a corresponding cost-reduction potential; from the outside it is often impossible to distinguish between them and a mullion-transom construction installed on site.

Shading mechanisms such as blinds or shutters are preferably inserted between the outside window pane and the TWD material. Lamella type systems can also be used in front of the facade, and display high working reliability when few movements take place between open and closed status or when in an always-lowered status.
2. as a heat insulating compound system with frameless direct installation. The transparently plastered capillary structures are supplied with a fabric for attaching the plaster to the conventional insulation, and fastened to the external wall with a black adhesive that serves as an absorber.

7.3 Heat storage by interior building elements

Heat storage by the interior components is decisive for the degree of the useful energy in both passive solar use by windows and in transparent heat insulating systems. Only if solar gains do not lead to overheating of the interior can the heating demand be reduced. The heat storage capacity of components can be roughly estimated from the storage mass, the thermal capacity and the possible rise in temperature of the storage mass. Thus, for example, a solid concrete wall with a thickness d of 30 cm, a heat capacity c of 1 kJ/kgK and a gross density ρ of 2100 kg/m^3 can store, with a rise in temperature of 5°C, an amount of heat of 0.875 kWh per square metre of surface.

$$\frac{Q}{A} = \rho\, d\, c\, \Delta T = 2100\frac{\text{kg}}{\text{m}^3}\times 0.3\text{m}\times 1.0\frac{\text{kJ}}{\text{kgK}}\times 5\text{K} = 3150\frac{\text{kJ}}{\text{m}^2} = 0.875\frac{\text{kWh}}{\text{m}^2} \qquad (7.18)$$

This view presupposes that the component is completely warmed or cooled to the temperature levels forming the basis of the calculation. This would presuppose very high heat transfer coefficients and high heat conductivities, which in practice is not the case. To what extent the storage capacity can be used depends, apart from the material values, primarily on the duration of a rise in temperature.

If, by dynamic calculation methods or by measurement, the amount of heat Q per surface A is determined which flows in a given period into the wall, then from this an effective thickness d_{eff} for the wall can be calculated, whose storage capability is fully used.

$$d_{eff} = \frac{Q}{A\, c\rho\Delta T} \qquad (7.19)$$

During a three-hour rise in temperature, a concrete wall (with A = 1 m^2 surface) can, largely irrespective of its thickness, take up approximately 33 Wh for each Kelvin of temperature rise (with heat take-up on both sides). This corresponds to an effective thickness of approximately 5 cm. With a six-hour rise in temperature this value is approximately 9 cm.

If the heating up of a room is to be calculated, then for rough estimates the amount of heat Q flowing into the component can be calculated via the heat transfer coefficient h_i and the temperature difference between the component surface $T_{s,1}$ (at the beginning of a time step Δt) and the room air T_i.

$$Q = h_i\, A\, \Delta t \left(T_i - T_{s,1}\right) \qquad (7.20)$$

After the time-step the new temperature of the component $T_{s,2}$ results from the stored amount of heat $Q_s = Q$:

$$T_{s,2} = T_{s,1} + \frac{Q_s}{A\,c\rho\,d_{eff}} \tag{7.21}$$

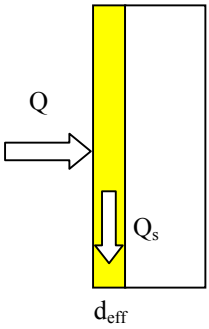

Figure 7.7: Amount of heat flowing into a component and the effective storage mass thickness d_{eff}.

This process is repeated with each time-step. For a more exact calculation of the temporally variable temperature distribution, an energy balance for a volume element of the storage mass must be created which leads to the classical thermal heat conduction equation. For simplicity, only one dimensional temperature distributions will be derived, i.e. from the air over the surface into the component depth.

For passive solar energy use the following boundary conditions play a role:

- the storage capacity of components during brief variations in temperature in the room caused by solar irradiance or air temperature modification,
- the potential for night cooling by utilisation of the periodic modification of the air temperature between day and night,
- the temperature amplitude and phase shift on the inner side of a transparently insulated wall.

In all cases heat is only absorbed or dissipated via the surface of the component. In the component interior there are no heat sources, so a very simple energy balance for each volume element results: from an entering heat flow $\dot{Q}_{in}$ by thermal conduction, part leads to the rise in temperature in the volume element (heat storage $\dot{Q}_{st}$), and the remainder is passed on by thermal conduction into the next element $\dot{Q}_{out}$.

$$\dot{Q}_{in} = \dot{Q}_{st} + \dot{Q}_{out} \tag{7.22}$$

The heat flow $\dot{Q}_{in}$ entering through surface A is, based on Fourier's law of thermal conduction, proportional to the temperature gradient at the point x_0.

$$\dot{Q}_{in} = -\lambda A \left.\frac{dT}{dx}\right|_{x_0} \tag{7.23}$$

The exiting heat flow $\dot{Q}_{out}$ at the point $x_0 + dx$ is, at constant heat conductivity λ, only different from $\dot{Q}_{in}$ if the temperature gradient has changed in the volume element, e.g. has become flatter during partial heat storage in the element.

$$\dot{Q}_{out} = -\lambda A \left.\frac{dT}{dx}\right|_{x_0+dx} \tag{7.24}$$

A Taylor series expansion of the temperature gradient at the point $x_0 + dx$ leads, if all higher-order members are ignored, to the following simplification:

$$\begin{aligned} \dot{Q}_{out} &= -\lambda A \left(\left.\frac{dT}{dx}\right|_{x_0} + \frac{d}{dx}\left(\left.\frac{dT}{dx}\right|_{x_0} \right) dx + \ldots \right) \\ &\approx -\lambda A \left(\left.\frac{dT}{dx}\right|_{x_0} + \left.\frac{d^2T}{dx^2}\right|_{x_0} dx \right) \end{aligned} \tag{7.25}$$

The amount of heat $\dot{Q}_{st}$ stored in the volume element $dV = A dx$ is given by

$$\dot{Q}_{st} = \rho \, dV \, c \frac{dT}{dt} \tag{7.26}$$

Thus the energy balance Equation (7.22) leads to:

$$\begin{aligned} -\lambda A \left.\frac{dT}{dx}\right|_{x_o} &= \rho dV c \frac{dT}{dt} - \lambda A \left.\frac{dT}{dx}\right|_{x_o} - \lambda A \left.\frac{d^2T}{dx^2}\right|_{x_o} dx \\ \frac{\lambda}{\rho c} \frac{d^2T}{dx^2} &= \frac{dT}{dt} \end{aligned} \tag{7.27}$$

where $a = \dfrac{\lambda}{\rho c} \left[\dfrac{m^2}{s}\right]$ is termed the thermal diffusivity; it lies between 10^{-7} m^2/s for wood and 10^{-4} m^2/s for metals.

7.3.1 Component temperatures for sudden temperature increases

With periodic boundary conditions or with temperature-equalising processes, the differential equation can be solved by a product approach, with one function dependent only on time and the other only on place.

If a temperature jump on one side is given as a boundary condition, an approach with the Gauss error integral (or error function *erf (z)*) leads to a more general solution than the product approach, since the initial temperature distribution *F(x)* at the point in time $t = 0$ can assume any values. The temperature and time functions are, however, no longer separate.

$$T(x,t) = \frac{1}{\sqrt{\pi}} \frac{1}{\sqrt{4at}} \int_{-\infty}^{+\infty} F(\xi) \exp\left(-\frac{(\xi - x)^2}{4at}\right) d\xi \tag{7.28}$$

From this general approach, some solutions for simple boundary conditions can be represented analytically. Thus for a concrete floor slab, the change in temperature at a certain depth (as an indication of the utilisation of the heat storage) as well as the heat flow occurring through the surface $\dot{Q}_{in}$ and the stored heat $\dot{Q}_{st}$ as a function of the duration of the temperature jump at the surface can be examined. Far more relevant in practice is the case of a temperature jump in the room air, which is transferred via convection to the component surface. This situation is very complex in its mathematical derivation and is therefore discussed later, with solutions given.

The temperature distribution for a component with a constant initial temperature T_c and a temperature jump at the component surface to zero for $t > 0$ is directly calculable from the Gauss error integral. With the substitution

$$\eta = \frac{\xi - x}{\sqrt{4at}} \qquad d\xi = d\eta\sqrt{4at} \qquad F(\xi) = T_c$$

the result from Equation (7.28) is:

$$\frac{T(x,t)}{T_c} = \frac{2}{\sqrt{\pi}} \int_0^{z=\frac{x}{\sqrt{4at}}} \exp\left(-\eta^2\right) d\eta = erf\left(\frac{x}{\sqrt{4at}}\right) = erf(z) \tag{7.29}$$

Factor 2 results from splitting the integral from Equation (7.28) into two parts and the symmetry of the function $\exp(-\eta^2)$. Strictly, the solution only applies to a semi-infinitely expanded body, but can also be used for shorter time intervals (a few hours) for a finitely expanded wall.

The error function *erf (z)* can be approximated with an error $< 2.5 \times 10^{-5}$ with an exponentially dampened polynomial function of third order (Wong, 1997).

With the auxiliary variable $p = \dfrac{1}{1 + 0.47047 \times z}$ the approximation equation reads

$$erf(z) = 1 - \left(0.3480242 \times p - 0.0958798 \times p^2 + 0.7478556 \times p^3\right) \times \exp\left(-z^2\right) \quad (7.30)$$

From the values of the error function one can directly determine which temperature *T(x, t)* prevails at any point *x* and time *t*. If, on the other hand, the penetration of a given temperature ratio *T(x,t)* to the initial temperature T_c at time *t* or depth *x* is to be determined, Equation (7.30) must be solved iteratively for *z*, and *x* and *t* must be calculated from $z = x/\sqrt{4at}$. The graphical representation of the error function for direct reading of the z-value from the function value $erf(z) = T(x,t)/T_c$ is represented below.

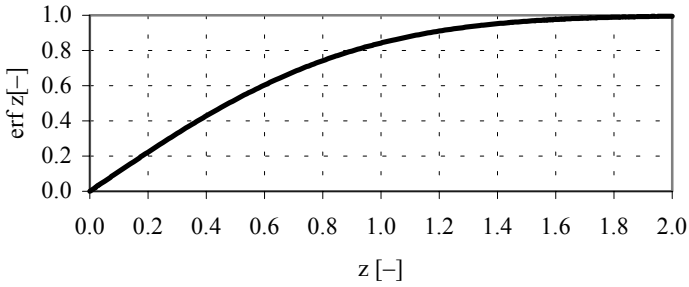

Figure 7.8: Error function $erf(z) = T(x,t)/T_c$ as a function of $z = x/\sqrt{4at}$.

The temperature jump must always take place from the initial temperature T_{c0} to the jump temperature $T_j = 0$°C. If this is not the case ($T_j \neq 0$), a standardised initial temperature T_c is calculated from the temperature difference of the initial temperature T_{c0} and the jump temperature T_j: $T_c = T_{c0} - T_j$. In what follows, the calculations are always based on a standardised initial temperature T_c and a surface temperature of zero.

Example 7.1

On a 20°C concrete (or wooden) floor, a surface temperature jump to $T_j = +30$°C occurs. Over what period of time has the temperature at a depth of 20 cm risen by 5°C?

	Heat conductivity λ [W/mK]	*Density* ρ [kg/m³]	*Heat capacity* c [kJ/kgK]	*Thermal diffusivity* a [m²/s]
Concrete	1.28	2200	0.879	0.66×10^{-6}
wood	0.2	700	2.4	0.12×10^{-6}

In order to adapt the boundary condition to a temperature jump of the surface temperature to 0°C, the initial floor temperature $T_{c0} = 20$°C is replaced by the standardised initial temperature $T_c = T_{c0} - T_j = 20$°C – 30°C = –10°C. A temperature rise *T*(*x*,*t*) of 5°C at a component depth of 20 cm thus corresponds to a temperature condition

$$\frac{T(x = 0.2m, t)}{T_c} = \frac{-5°C}{-10°C} = 0.5 = erf(z)$$

The iteratively calculated z-value (which can also be read off Figure 7.8) is $z = 0.477 = \frac{x}{\sqrt{4at}}$. From $t = \frac{x^2}{4a\,z^2}$ the result for the concrete ceiling is a temperature-rise time of 18.5 hours, and for the wooden ceiling 111 hours.

If the temperature ratio $T(x,t)/T_c = erf(z)$ is represented as a function of time, it can be seen how quickly a surface temperature jump propagates into the component. For $x > 0$ the temperature at $t = 0$ is at first the constant initial temperature T_c and the temperature ratio is unity. With increasing time, the component temperature approaches the surface temperature of zero, i.e. the temperature ratio tends towards zero.

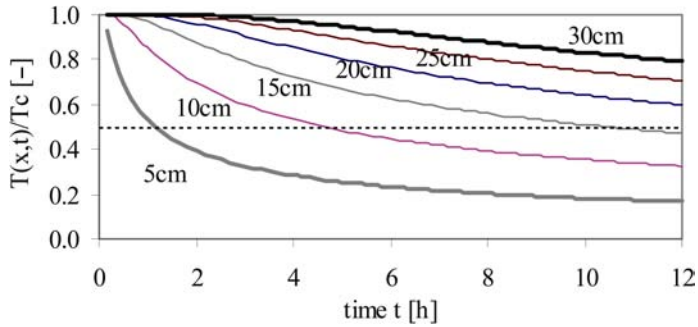

Figure 7.9: Error function $erf(z) = T(x,t)/T_c$ as a function of time for concrete floors with thermal diffusivity $a = 0.66 \times 10^{-6} m^2/s$.

After 12 hours, half of the surface temperature increase ($T(x,t)/T_c = 0.5$) is at a component depth of 16 cm for the concrete floor, which illustrates the limitation of the effectively usable storage capacity. Only with times >> 12 hours does the component temperature approach the surface value of zero ($T(x,t)/T_c \rightarrow 0$).

For wood with a lower thermal diffusivity a, a surface temperature jump clearly continues more slowly.

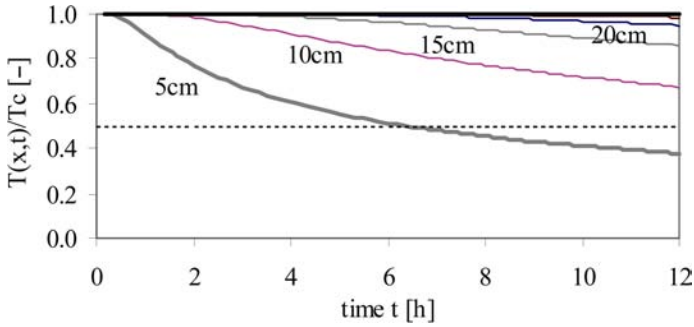

Figure 7.10: Temperature field in the component wood as a function of time.

After 12 hours, half of the surface temperature increase has only reached a depth of 7 cm. For component thicknesses over 20 cm, the temperature has not changed even after 12 hours.

The heat flow *dQ/dt* entering or leaving the surface *A* is proportional, based on Fourier's law, to the temperature gradient at the surface:

$$\begin{aligned}\frac{dQ}{dt} &= -\lambda A \left.\frac{dT}{dx}\right|_{x=0} = -\lambda A T_c \left.\frac{d}{dx} erf\left(\frac{x}{\sqrt{4at}}\right)\right|_{x=0} \\ &= -\lambda A T_c \frac{1}{\sqrt{4at}} \frac{2}{\sqrt{\pi}} \underbrace{\exp\left(-\frac{x^2}{4at}\right)}_{=1 \quad für\ x=0} = -A \underbrace{\sqrt{\lambda\rho c}}_{b} \sqrt{\frac{1}{\pi}} T_c \frac{1}{\sqrt{t}}\end{aligned} \tag{7.31}$$

The heat flow is proportional to the so-called heat penetration coefficient $b = \sqrt{\lambda\rho c}$ and falls with $1/\sqrt{t}$.

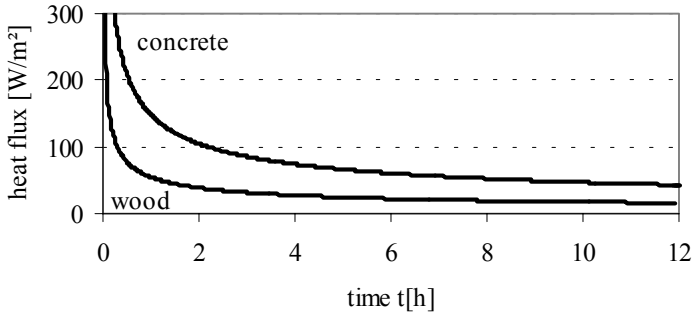

Figure 7.11: Heat flux as a function of time for a concrete and a wooden floor with a 10 K temperature jump.

The integration of the heat flow over time results in the total amount of heat penetrating into the component when there is a surface temperature jump.

$$\frac{Q}{A} = \int \frac{dQ}{A} = \int_0^{t_0} \left(-\sqrt{\frac{\lambda\rho c}{\pi}} T_c \frac{1}{\sqrt{t}}\right) dt = -\frac{2}{\sqrt{\pi}} \underbrace{\sqrt{\lambda\rho c}}_{b} \sqrt{t_0} T_c \tag{7.32}$$

Since the surface temperature for $t > 0$ has been set by definition to 0°C, for T_c the standardised initial temperature must be used again.

Example 7.2

Calculation of the amount of heat penetrating a component with a temperature jump at the surface of 10K for t_0 = 12h for the two floors from Example 7.1.

The heat penetration coefficient $b = \sqrt{\lambda \rho c}$ for concrete is $1.573\ \mathrm{kJ/(m^2K\sqrt{s})}$, and for wood it is $0.579\ \mathrm{kJ/(m^2K\sqrt{s})}$. Thus within 12 hours an amount of heat of 3689 kJ/m² = 1.02 kWh/m² is brought into the concrete ceiling and 0.38 kWh/m² into the wooden ceiling.

The amount of energy stored within a component is, like the heat flow, directly proportional to the heat penetration coefficient b and to the temperature jump ΔT at the surface, but it rises with the root of time.

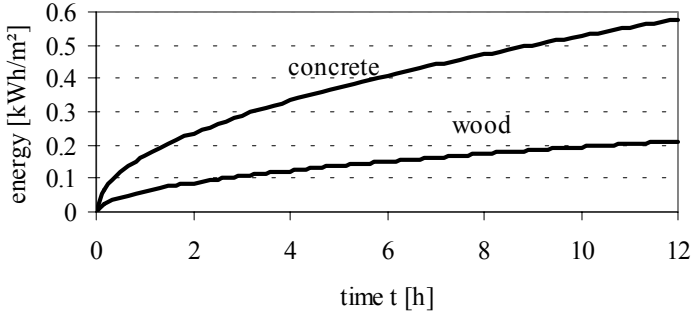

Figure 7.12: Amount of energy led into the component with a rise in temperature at the surface of 10K.

Usually, however, it is not the surface temperature but the air temperature which is known. Between the air and the surface temperature change there is a phase shift and a dampening of the amplitude. At a given air temperature T_o and a given heat transfer coefficient h between the air and the surface, the temperature field $T(x,t)$ can be calculated as follows (Gröber, 1988):

$$\frac{T(t,x)}{T_c} = erf\left(\frac{x}{\sqrt{4at}}\right) + \exp\left(at\left(\frac{h}{\lambda}\right)^2 + \frac{h}{\lambda}x\right)\left(1 - erf\left(\frac{x}{\sqrt{4at}} + \frac{h}{\lambda}\sqrt{at}\right)\right) \qquad (7.33)$$

At the surface $x = 0$, therefore, the following temperature appears:

$$T(t, x=0) = T_c \exp\left(at\left(\frac{h}{\lambda}\right)^2\right)\left(1 - erf\left(\frac{h}{\lambda}\sqrt{at}\right)\right) \qquad (7.34)$$

Example 7.3

Calculation of the temperature of a concrete ceiling at the surface and at a depth of 5 cm for t = 1 h and t = 10 h with parameters from Example 7.1, if the air temperature, rather than the surface temperature, jumps to 30°C. The heat transfer coefficient h is 8 W/m²K.

First the surface temperature is calculated for $x = 0$ using Equation (7.33). For $t = 1\ h$ the temperature at the surface is:

$$T(t = 1\ h, x = 0)/T_c = 0.73$$

with

$$\exp\left(at\left(\frac{h}{\lambda}\right)^2\right) = \exp\left(\underbrace{0.66\times10^{-6}\frac{m^2}{s}\times 1\ h\times 3600\frac{s}{h}}_{0.0928}\times\left(\frac{8\frac{W}{m^2K}}{1.28\frac{W}{mK}}\right)^2\right) = 1.097$$

and

$$erf\left(\frac{h}{\lambda}\sqrt{at}\right) = erf\left(0.304\right) = 0.33$$

With an air temperature jump of 10 K, the ratio of the surface temperature to the initial body temperature T_c after one hour is still at 73%, i.e. with the selected boundary condition for heating, the surface temperature has increased by (1–0.73) × 10 K = 2.7 K . After t = 10 h the temperature ratio is 43.8%. The surface temperature has then increased by 5.6 K.

At a depth of 5 cm, the temperature ratio after t = 1 h is 0.903, i.e. the temperature has only increased by 1 K. After 10 hours the temperature at a depth of 5 cm has increased by 4.33 K.

With air temperature modifications, the potential for heat storage with a limited duration of the temperature jump is clearly smaller than with direct impact of the temperature jump on the surface. After 12 hours the surface has only taken up 60% of the air temperature jump, i.e. the effective storage capacity sinks by 40%.

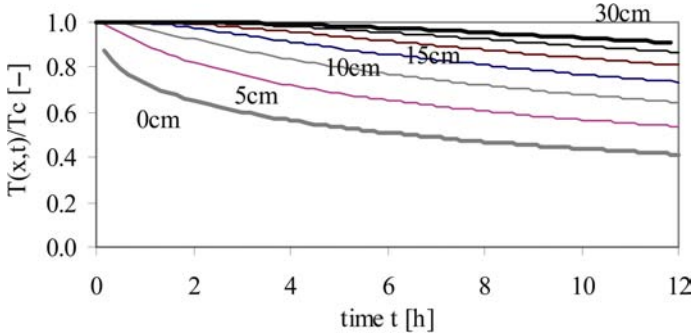

Figure 7.13: Temperature ratio as a function of time at a given air temperature for the material concrete.

The surface temperature changes during an air temperature jump essentially depend on the relation of the heat transfer coefficient h_i to the heat conductivity λ of the component. Component surfaces of materials with low heat conductivity clearly assume the air temperature faster (i.e. $T(x = 0,t)/T_c$ becomes zero) than components which conduct heat well. Deep in the component, on the other hand, a temperature jump of air continues only very slowly with poorly conducting materials.

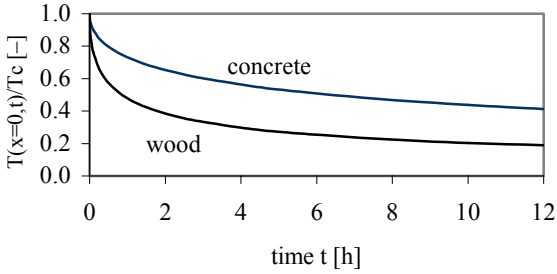

Figure 7.14: Relation of the surface temperature to the initial body temperature during an air temperature jump of 10 K.

The heat flow density into the component can be obtained either from:

$$\frac{\dot{Q}}{A} = h_i \left(T_o - T_{x=0}\right) \qquad \text{or} \qquad \frac{\dot{Q}}{A} = -\lambda \left.\frac{\partial T}{\partial x}\right|_{x=0}$$

with the common solution for an air temperature jump T_o to zero:

$$\frac{\dot{Q}}{A} = -h_i T_c \exp\left(\left(\frac{h}{\lambda}\right)^2 at\right)\left(1 - erf\left(\left(\frac{h}{\lambda}\right)\sqrt{at}\right)\right) \tag{7.35}$$

Since the temperature difference of the surface $T(x = 0)$ and air T_o (here zero) is larger at the concrete surface than at the wood surface, the larger heat flows and stored amounts of energy occur there.

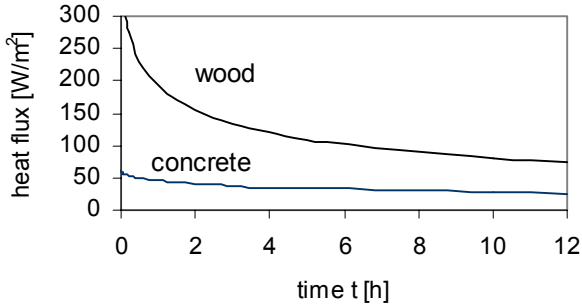

Figure 7.15: Heat flux into wood and concrete at an air temperature jump of 10 K.

To calculate the amount of heat Q for each unit area A which has flowed into the component till the point in time t_1, the heat flux density $\dot{Q}/A$ must be integrated over the time. A solution to this problem is probably very complex. It is simpler to calculate the heat flow density in smaller time intervals and total afterwards.

$$\frac{Q}{A} = \frac{1}{A}\int_0^{t_1} \dot{Q}dt \approx \frac{1}{A}\sum_1^n \dot{Q}_i \Delta t \quad \text{with} = \frac{t_1}{\Delta t} \tag{7.36}$$

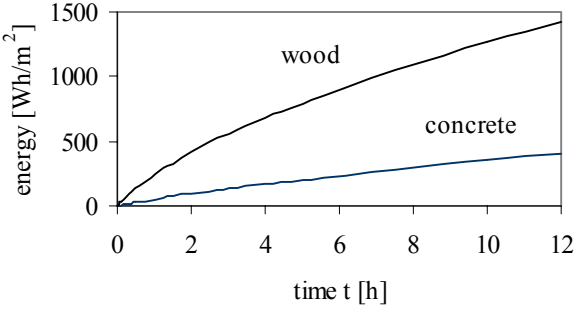

Figure 7.16: Amount of heat stored in the materials on an air temperature jump of 10 K.

7.3.2 Periodically variable temperatures

Apart from temperature jumps, for practical applications periodic changes in temperature caused by the external climate are of particular importance. The outside temperature T_o and the irradiance converted to a fictitious sol-air temperature can be approximated as periodic functions of time t with a period t_0 of 24 hours and an amplitude T_{om}.

The analytic solution of the thermal conduction equation is, as with the temperature jump, simpler for a periodic boundary condition at the surface. Firstly, therefore, the material temperatures of a semi-infinitely expanded component with periodically varying surface temperatures $T_s(t)$ will be calculated, and only afterwards will they be generalised to the boundary condition of the air temperature. With a period duration t_0 and an amplitude T_{sm}, the surface temperature $T_s(t)$ is set as follows:

$$T_s(t) = T_{sm} \cos\left(\frac{2\pi}{t_0} t\right) \tag{7.37}$$

Proceeding from a product approach for the temperature field $T(t,x) = \varphi(t)\psi(x)$, for the time function $\varphi(t)$ the complex exponential function $\exp(ipt) = \cos(pt) + i\sin(pt)$ is selected as the periodic function. With this approach for the time function and $d\varphi(t)/dt = ip\exp(ipt)$, the thermal conduction equation $a\frac{d^2T}{dx^2} = \frac{dT}{dt}$ becomes

$$a\frac{d^2\Psi(x)}{dx^2}\exp(ipt)-ip\psi(x)\exp(ipt)=0$$
$$\Leftrightarrow \frac{d^2\Psi(x)}{dx^2}-i\frac{p}{a}\psi(x)=0 \tag{7.38}$$

with the solution

$$\psi(x)=C\exp\left(x\sqrt{-i\frac{p}{a}}\right) \tag{7.39}$$

and

$$T(t,x)=C\exp(ipt)\exp\left(x\sqrt{-i\frac{p}{a}}\right) \tag{7.40}$$

which can be split into a real and an imaginary part. After some rearrangements and use of the surface boundary condition at $x = 0$, the constant of the imaginary solution becomes zero and the real temperature field is

$$T(x,t)=T_{sm}\exp\left(-x\sqrt{\frac{\pi}{at_0}}\right)\cos\left(\frac{2\pi}{t_0}t-x\sqrt{\frac{\pi}{at_0}}\right) \tag{7.41}$$

The wavelength x_l of the cosine function results in $x_l=2\sqrt{\pi a t_0}$ from the relationship $x_l\sqrt{\pi/(at_0)}=2\pi$, and the propagation rate of the wave is $v=x_0/t_0=2\sqrt{\pi a/t_0}$. The subsiding exponential function dampens the amplitude of the wave with rising x. The temporal phase shift t_x of the temperature wave at component depth x compared to the surface $x = 0$ is

$$\frac{2\pi}{t_0}t_x=x\sqrt{\frac{\pi}{at_0}}\Rightarrow t_x=\frac{x}{2}\sqrt{\frac{t_0}{a\pi}} \tag{7.42}$$

A periodic change in temperature at a component surface is seen in transparently insulated components in which the absorption of solar radiation on the wall surface leads to a periodic change in temperature.

With Equation (7.41) the periodic change in temperature within the component can be calculated with exponentially dampened amplitude and period duration t_0. The temperature field $T(x,t)$ is related for illustration purposes to the amplitude of the surface temperature fluctuation T_{sm}. Even at just 5 cm component depth, the surface amplitude of a concrete wall is reduced by 30%. The phase shift between the maximum surface temperature and the temperature at a depth of 5 cm is 1.5 h.

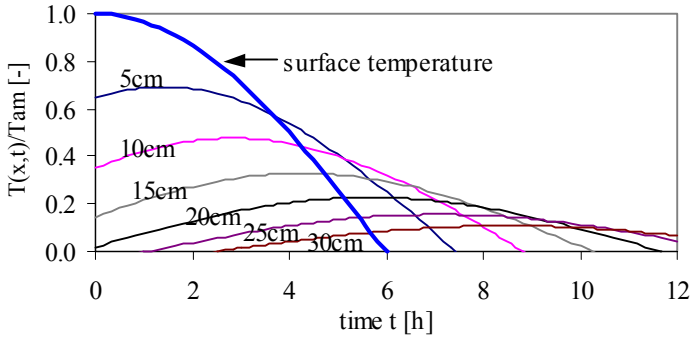

Figure 7.17: Variation in temperature $T(x, t)$ normalised to the amplitude T_{sm} around the average value as a function of time and component depth x in 5 cm steps for a concrete building component.

Example 7.4

On a solid wall with transparent thermal insulation, the absorber temperatures reaches 50°C during the day and falls to 10°C at night. To which value has the amplitude dropped after 24 cm (38 cm) wall thickness and after how many hours has the amplitude reached x = 0.24 m (0.38 m)? The thermal diffusivity a of the wall is 0.66×10^{-6} m^2/s.

The phase shift between the maximum surface temperature and maximum temperature at 24 cm (38 cm) wall thickness is

$$t_x = \frac{0.24m}{2}\sqrt{\frac{24h \times 3600\frac{s}{h}}{0.66\times10^{-6}\frac{m^2}{s}\times\pi}} = 6.8h$$

and 10.8 h with 0.38 m wall thickness. The amplitude ratio is

$$\frac{T(x,t)}{T_{sm}} = \exp\left(-0.24m\sqrt{\frac{\pi}{0.66\times10^{-6}\frac{m^2}{s}\times 24h\times3600\frac{s}{h}}}\right) = 0.17$$

for the 24-cm wall and 0.06 for the 38-cm wall. The temperature amplitude, which amounts to 20 K around the average value of 30°C, is dampened to 3.4°C and 1.2°C respectively.

The heat flow into a component with a periodic temperature boundary condition is again calculated, using Fourier's law, from the temperature gradient at the surface:

$$\frac{dQ}{dt} = -\lambda A \left.\frac{dT}{dx}\right|_{x=0} = -\lambda A \frac{d}{dx}\left(T_{sm} \exp\left(-x\sqrt{\frac{\pi}{at_0}}\right)\cos\left(\frac{2\pi}{t_0}t - x\sqrt{\frac{\pi}{at_0}}\right)\right)\Bigg|_{x=0}$$

$$= -\lambda A T_{sm} \left[\begin{array}{l} \underbrace{\exp\left(-x\sqrt{\frac{\pi}{at_0}}\right)}_{1} \times -\sqrt{\frac{\pi}{at_0}} \times \cos\left(\frac{2\pi}{t_0}t - \underbrace{x\sqrt{\frac{\pi}{at_0}}}_{0}\right) \\ + \underbrace{\exp\left(-x\sqrt{\frac{\pi}{at_0}}\right)}_{1} \times -\sin\left(\frac{2\pi}{t_0}t - \underbrace{x\sqrt{\frac{\pi}{at_0}}}_{0}\right) \times -\sqrt{\frac{\pi}{at_0}} \end{array} \right]_{x=0} \tag{7.43}$$

$$= \lambda A T_{sm} \sqrt{\frac{\pi}{at_0}} \left(\cos\left(\frac{2\pi}{t_0}t\right) - \sin\left(\frac{2\pi}{t_0}t\right)\right)$$

The heat flow $\dot{Q}/A$ is proportional to the surface temperature amplitude T_{sm}.

Example 7.5

A building with concrete ceilings is to be passively cooled by night ventilation. The surface temperatures can be approximated with a cosine function with an average value of 22°C, a maximum deviation of ±5°C and a period duration $t_0 = 24$ h.

The heat flow removed, based on Equation (7.43), is a maximum of –67 W/m^2 with a phase shift to the temperature of $t_0/8$, i.e. 3 hours.

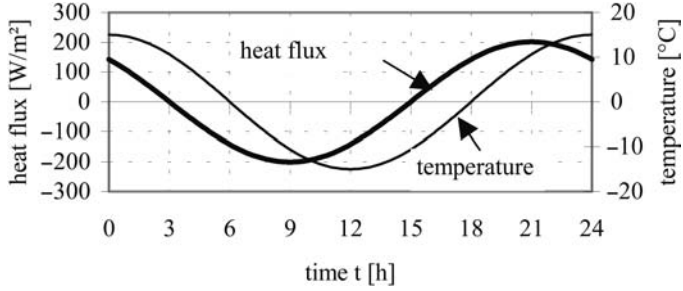

Figure 7.18: Heat flux into a concrete ceiling with a periodic surface temperature at amplitude $T_{sm} = 5$°C.

The integration of the heat flux results in the surface-related energy Q/A. If the stored or removed amount of heat is to be calculated, the integration limits t_1 and t_2 must be selected in such a way that only positive or negative heat flows are integrated. From Example 7.5 it can be seen that between the maximum heat flow and maximum surface temperature a phase shift of π/4 exists, i.e. one-eighth of a period.

$$\frac{Q}{A} = \lambda T_{sm}\sqrt{\frac{\pi}{at_0}}\int_{t_1}^{t_2}\left(\cos\left(\frac{2\pi}{t_0}t\right)-\sin\left(\frac{2\pi}{t_0}t\right)\right)dt$$
$$= \lambda T_{sm}\sqrt{\frac{\pi}{at_0}}\frac{t_0}{2\pi}\left(\sin\left(\frac{2\pi t_2}{t_0}\right)-\sin\left(\frac{2\pi t_1}{t_0}\right)+\cos\left(\frac{2\pi t_2}{t_0}\right)-\cos\left(\frac{2\pi t_1}{t_0}\right)\right) \quad (7.44)$$

The stored amount of heat of a half period results from the integral of the positive heat flows with a lower integration limit of $t_1 = 5/8\ t_0$ and an upper limit $t_2 = 5/8\ t_0 + t_0/2$, the released amount of heat from the integral being between $t_1 = t_0/8$ and $5/8\ t_0$.

Example 7.6

Calculation of the energy removed in a half period (12 h) by night cooling with a surface temperature amplitude of 5 K.

From Equation (7.44) the result is an amount of energy removed by night cooling of –0.51 kWh/m^2 at a lower integration limit of $t_1 = t_0/8$.

Normally it is not the surface temperature T_s which is known, but only the air temperature T_o with amplitude T_{om} and the heat transfer coefficient h between the air and the surface. The analytic solution corresponds to the solution with the surface temperature as a boundary condition from Equation (7.41), with the amplitude dampened by a factor η_0 and a phase shift ε_0 occurring due to thermal resistance between the air and the surface.

$$T(x,t) = T_{om}\eta_0 \exp\left(-x\sqrt{\frac{\pi}{at_0}}\right)\cos\left(\frac{2\pi}{t_0}t-\left(\varepsilon_0 + x\sqrt{\frac{\pi}{at_0}}\right)\right) \quad (7.45)$$

with

$$\eta_0 = \sqrt{\left(1+2\sqrt{\frac{\pi}{(h/\lambda)^2 at_0}}+2\frac{\pi}{(h/\lambda)^2 at_0}\right)^{-1}}$$

and

$$\varepsilon_0 = \arctan\left(\left(1+\sqrt{\frac{(h/\lambda)^2 at_0}{\pi}}\right)^{-1}\right)$$

At $x = 0$ the surface temperature T_s is obtained with amplitude dampening η_0 and phase shift ε_0.

$$T(x=0,t) = T_s = T_{om}\eta_0\cos\left(\frac{2\pi}{t_0}t-\varepsilon_0\right) \quad (7.46)$$

Example 7.7

Calculation of the surface temperature amplitude and the phase shift ε_0 for the concrete ceiling in Example 7.5, with a heat transfer coefficient h = 8 W/m²K. The air temperature is to have an amplitude of ±5 K around an average value of 22°C.

With

$$\frac{\pi}{(h/\lambda)^2 at_0} = \frac{\pi}{\left(8\frac{W}{m^2K}/1.28\frac{W}{mK}\right)^2 0.66\times10^{-6}\frac{m^2}{s}\times24h\times3600\frac{s}{h}} = 1.41$$

the result is

$$\eta_0 = \sqrt{\frac{1}{1+2\sqrt{1.41}+2\times1.41}} = 0.4$$

The maximum temperature amplitude at the surface is now only $T_s = 5K\times0.4 = 2K$, and thus the removable energy falls by 60%! The phase shift is

$$\varepsilon_0 = \arctan\left(\left(1+\sqrt{\frac{1}{1.41}}\right)^{-1}\right) = 28.5°$$, i.e. in a 24 h period scarcely 2 h.

7.3.3 Influence of solar irradiance

If, in addition to air temperature fluctuations, the irradiance on a component surface is also to be considered, the use of a simple energy balance model is recommended, with which the short-wave solar irradiance is converted into a so-called sol-air temperature. With the help of the sol-air temperature, the analytic solutions of the thermal conduction equation already discussed can then be used.

The heat flow supplied to a component surface consists of the absorbed irradiance αG plus the heat flow transferred by the air (temperature T_o) to the surface (T_s) with the heat transfer coefficient h. This supplied heat flow is combined in a simple model, ignoring temperature-dependent modifications of the heat transfer coefficient h, into a purely temperature-dependent heat flow described by the sol-air temperature T_{So}.

$$\begin{aligned} \alpha G + h(T_o - T_s) &= h(T_{So} - T_s) \\ T_{So} &= T_o + \frac{\alpha G}{h} \end{aligned} \tag{7.47}$$

With the sol-air temperature T_{So}, the heat storage in components can then be calculated with the solutions of the thermal conduction equation already considered.

Example 7.8

Calculation of the sol-air temperature and the energy stored in a concrete floor, with periodically varying irradiance at an amplitude of 500 W/m^2 and period t_0 = 24 h transmitted through the windows, an absorption coefficient of the floor of $\alpha = 0.6$, a room air and ceiling average temperature T_o = 20°C and a heat transfer coefficient h = 8 W/m^{2}K. The maximum sol-air temperature is:

$$T_{So,\max} = 20°C + \frac{0.6 \times 500 \frac{W}{m^2}}{8 \frac{W}{m^2 K}} = 57.5°C$$

Via the fictitious sol-air temperature, first the surface temperature at the concrete surface is calculated, and from this, using Equation (7.44), the stored energy per square metre of surface.

Using Example 7.7, $\eta_0 = 0.4$ and thus the maximum air temperature fluctuation of 57.5°C – 20°C = 37.5°C is reduced to a maximum surface temperature fluctuation of $T_{a,max} = \eta_0 (T_{So,max} - T_o)$ = 15°C. The energy stored during a half period is 1.54 kWh/m^2.

Altogether, however, an irradiance of $\int_0^{t_0/2} G dt = G_{\max} \int_0^{t_0/2} \sin\left(2\pi \frac{t}{t_0}\right) dt = \frac{G_{\max} t_0}{\pi} = 3.8 \frac{kWh}{m^2}$ is transmitted through the glazing during the half period, and of it 60%, i.e. 2.3 kWh/m^2, is absorbed by the concrete floor. The difference between the absorbed irradiance and stored heat has been transferred over the heat transfer coefficient h directly to the room air.